Journal of the European Ceramic Society **17** (1997) 1729–1739

PII: S0955-2219(97)00036-8
0955-2219/97/$17.00

Effect of Grain Size on the Kinetics of Isothermal Tetragonal to Monoclinic Transformation in ZrO_2(2 mol% Y_2O_3) Ceramics

W. Z. Zhu & M. Yan

Department of Materials Science and Engineering, Zhejing University, Hangzhou, 310027, PR China

(Received 30 July 1996; revised version received 2 January 1997; accepted 10 February 1997)

Abstract

In this paper, effect of grain size on kinetics of isothermal tetragonal(t) to monoclinic(m) transformation in ZrO_2(2mol% Y_2O_3) ceramics has been studied by means of thermal expansion analysis (TEA), X-ray diffraction (XRD), scanning electron microscopy (SEM) and transmission electron microscopy (TEM). Experimental results reveal that t→m transformation in ZrO_2(Y_2O_3) ceramics is essentially isothermal with its time temperature transformation (TTT) curve expressed in the form of C-shape, occurrence of which has been analyzed in terms of nucleation and growth process. Grain size has been shown to have significant effect on the isothermal kinetics of t→m transition. With decreasing grain size of t-phase, the "nose" temperature of the TTT curve is decreased and incubation period is shortened. However, the incompleteness of the transformation is enhanced due to higher transformation activation energy. TEM observation also indicates that phase constituents may vary with grain size with the implication of the effect of grain size on the stability of t-phase.

1 Introduction

It is well documented that stress-assisted tetragonal(t) to monoclinic(m) transformation in ZrO_2 alloys is the origin of toughening, in that stress concentration at the tip of a propagating crack can obviously be relaxed through dilational transformation.[1–5] The nature of t→m transformation is usually considered to be athermal, but may also show some isothermal character which has received relatively little attention. It is proposed that kinetics of isothermal t→m transition in ZrO_2(Y_2O_3) ceramics might be controlled by the short- range diffusion of oxygen vacancies produced due to the substitution of yttrium ions for zirconium ions to keep electrical neutrality.[6–8] However, a thermally activated mechanism is also suggested to account for this time-dependent feature in accordance with the conventional isothermal martensitic transformation in metallic alloys,[9–10] namely, there exists a linear relationship between critical nucleation energy barrier and degree of supercooling, and the kinetics of transformation is totally controlled by nucleation. To our knowledge, no experimental evidence has been obtained to support the viewpoint of isothermal martensitic character. It is well clarified experimentally that t→m transition in pure zirconia is an athermal martensitic transformation in that the amount of *m*-phase is solely determined by the degree of supercooling,[11–13] while the mechanism of t→m transition in yttria-containing zirconia remains to be studied both theoretically and experimentally. In this paper, the effect of grain size on kinetics of isothermal t→m transformation in ZrO_2(2 mol% Y_2O_3) ceramics has been studied by intentionally choosing two typical materials, (i.e. fine-grained material and coarse-grained material) in an attempt to gain insight into the kinetics nature of this transition.

2 Experimental procedure

Zirconia powders containing 2 mol% yttria in solid solution were prepared by a coprecipitation technique, in which starting materials used were 99·9%

pure Y_2O_3 and 99·7% pure $ZrOCl_2.8H_2O$ oxide. Y_2O_3 was dissolved in a hot HCl solution and the $ZrOCl_2.8H_2O$ was dissolved in distilled water. A solution of NH_4OH(10 wt%) and a mixture of YCl_3 and $ZrOCl_2$ solution were simultaneously added to a beaker to form gel-like hydroxide precipitates by controlling the PH value above 11. After filtration, the precipitates were dried in an oven at 70°C. Dried precipitates were calcined in an air furnance at 650°C for 2 h. The calcined powders were cold-pressed into pellets of 24 cm × 6 cm × 6 cm in size under the pressure of 300 MPa. Up to 70% theoretical density could be obtained in forming the green bulk. The pellets were sintered at 1400 and 1600°C respectively with 5 h as holding time followed by furnace cooling and almost full density was achieved. For simplicity, the specimen sintered at 1600°C was donated as 2Y(1600), correspondingly, specimen sintered at 1400°C was donated as 2Y(1400). A linear interception method was adopted to measure the grain size, which is the statistical average value of at least 50 grains. The surface morphology was observed on Hitachi S-570 type scanning electron microscopy, before which a thin film of gold was coated on the specimen. The experiment of thermal expansion analysis was performed using a Perkin-Elmer 7 Series Thermal Analysis System with a sample machined to the size 3 mm × 3 mm × 4 mm. On the thermal expansion curve, the point at which the tangential line deviates from the curve was defined as transformation temperature. The volume fraction of the monoclinic phase was calculated using the following formula suggested by Garvie:[14]

$$M\% = \frac{I_m(11\bar{1}) + I_m(111)}{I_m(11\bar{1}) + I_{ct}(111) + I_m(111)} \times 100\% \quad (1)$$

where $I_m(11\bar{1})$ and $I_m(111)$ refer to the relative intensity of the $(11\bar{1})$ and (111) planes of the monoclinic phase, respectively; and $I_{ct}(111)$ refers to the relative intensity of the (111) plane of the tetragonal or cubic phase. The sample for the transmission electron microscope was prepared by the conventional agron-ion thinning to perforation followed by the procedure of applying a thin film of amorphous carbon, while observation was made using a Hitachi H-800 microscope operated at 200 KV.

3 Results and discussion

3.1 Thermal expansion curves of specimens with different grain size

Scanning electron microscopy photographs of natural surfaces of ZrO_2 (2 mol%Y_2O_3) ceramics pressurelessly sintered at 1600°C and 1400°C, respectively, are shown in Fig. 1 from which corresponding average grain sizes of 1·47 μm and 0·48 μm are obtained, in addition, relative density of more than 98% can be achieved. Figure 2 shows thermal expansion curves of two samples obtained at a heating and cooling rate of 10°C min^{-1}. It is clear that at initial heating, increase of sample size results from increase in temperature, namely, linear expansion. When the temperature is increased over A_s point (starting temperature of m→t transition), the sample size decreases drastically due to volume shrinkage arising from m→t transformation. A further increase of temperature over A_f point (ending temperature of m→t transition) means that curves reverse to linear expansion section indicating that at temperatures above A_f, only t phase exists in samples. Conversely, linear shrinkage caused by a decrease in temperature is observed at initial cooling. When temperature is decreased

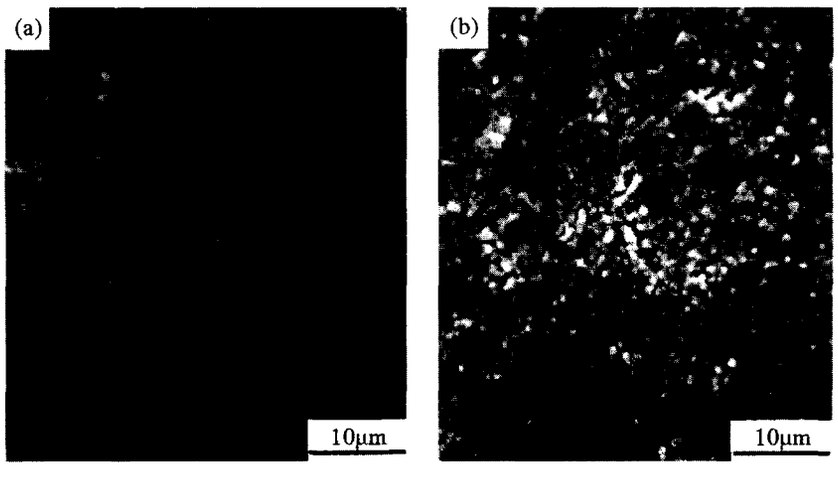

Fig. 1. SEM photographs of natural surfaces of ZrO_2 (2mol%Y_2O_3) ceramics sintered at different temperatures: (a) 1600°C; (b) 1400°C.

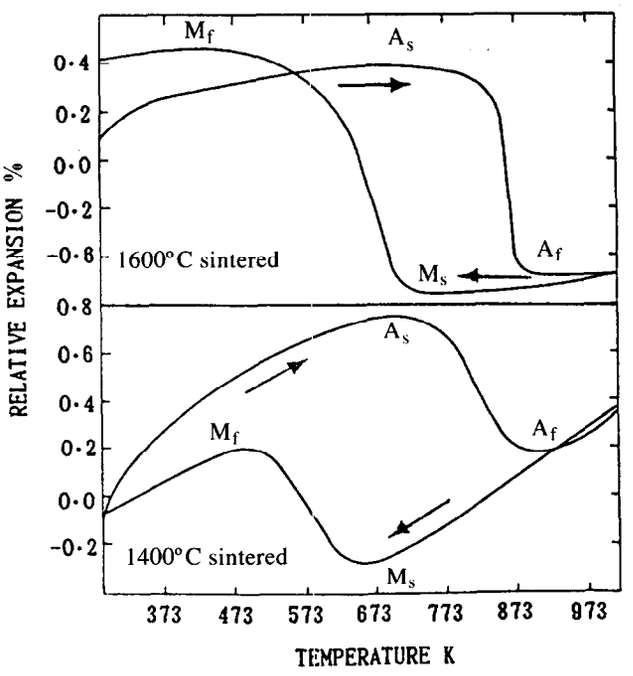

Fig. 2. Thermal expansion curves obtained at a heating and cooling rate of 10°C min^{-1} for ZrO_2 (2mol%Y_2O_3) ceramics sintered at different temperatures.

below M_s point (starting temperature of $t \rightarrow m$ transition), the sample size increases evidently due to the dilational effect of t→m transformation. Upon further decreasing the temperature below M_f point (ending temperature of t→m transformation) curves again reverse to linear shrinkage section. Grain size has an obvious effect on starting temperatures of t→m and m→t transformations in that the larger the grain size, the higher the M_s and A_s points, the larger the thermal expansion volume arising from t→m transition as well as volume fraction of m-phase produced. Table 1 lists starting and ending temperatures of t→m and m→t transitions for ZrO_2(2 mol%Y_2O_3) specimens sintered at different temperatures.

3.2 Effect of grain size on kinetics of isothermal t→m transition

In order to obtain kinetics data of isothermal t→m transition, isothermal thermal expansion analysis has been carried out for specimens with different grain size. Thermal expansion curves obtained at a heating and cooling rate of 100°C min^{-1} for two different specimens held at 350°C for 4 h are shown in Fig. 3 in which (a) and (b) refer to curves of expansion versus temperature and expansion versus time, respectively. On the curves, the ab section represents linear expansion solely caused by increase in temperature; the bc section indicates decrease of specimen size resulting from m→t transition; the cd section represents linear expansion after the temperature is increased over A_f point; de section refers to linear shrinkage during cooling; the ef section represents increase in specimen size due to t→m transition before and during holding; the fg section refers to increase in specimen size caused by t→m transformation resulting from further cooling after holding is over; the gh section represents linear shrinkage during cooling to room temperature. Each section on curve of expansion versus temperature corresponds exactly to one on curve of expansion versus time and shape of curve held at other temperatures is similar to one just indicated. Volume fraction of *m*-phase and thermal expansion for 2Y(1600) and 2Y(1400) specimens are tabulated in Tables 2 and 3, respectively. It is evident from the tables that a cooling rate of 100°C min^{-1} is not high enough to inhibit the production of *m*-phase before holding (pre-*m* phase). The lower the holding temperature, the larger the volume fraction of pre-*m* phase, which leads to the fact that initial phase constitutents prior to holding for the measurement of isothermal kinetics are *t* plus *m* dual phase and some *t*-phase transforms to *m* phase during holding thereafter. Changes of fraction of m-phase with holding time for 2Y(1600) and 2Y(1400) specimens held at different temperatures are shown in Fig. 4 and corresponding time-temperature-transformation(TTT) curves are illustrated in Fig. 5. The isothermal transition possesses the following features:

Table 1. Starting and ending temperatures of t→m and m→t transition for ZrO_2(2mol% Y_2O_3) specimens sintered at different temperatures

Temperature	*Grain size*	M_s	M_f	A_s	A_f
1600°C	1·47 μm	459°C	322°C	567°C	602°C
1400°C	0·48 μm	374°C	226°C	454°C	620°C

(1) The existence of an incubation period which initially becomes shorter with decreasing holding temperature, then becomes longer when the holding temperature is further decreased, resulting in the appearance of a 'nose' temperature as well as C-shaped curve. The existence of an incubation period is one of the characteristics of diffusional transformation whose isothermal kinetics can be expressed in terms of Avrami equation, i.e. $f = 1 - exp(-kt^n)$, where f is the volume fraction of the transformed phase, k is a variable associated with the energy barrier for critical nucleation and growth, and n is a constant depending on the nucleation sites.

(2) The 'nose' temperature for 2Y(1600) specimen is 400°C while that for 2Y(1400) specimen is

300°C with the implication that the smaller the grain size, the lower the 'nose' temperature. By comparing Figs 5(a) and (b), it is noted that the incubation period of the fine-grained specimen is shorter than that of the coarse-grained specimen and the TTT curve of the fine grained specimen lies to the down-left side of the coarse grained specimen.

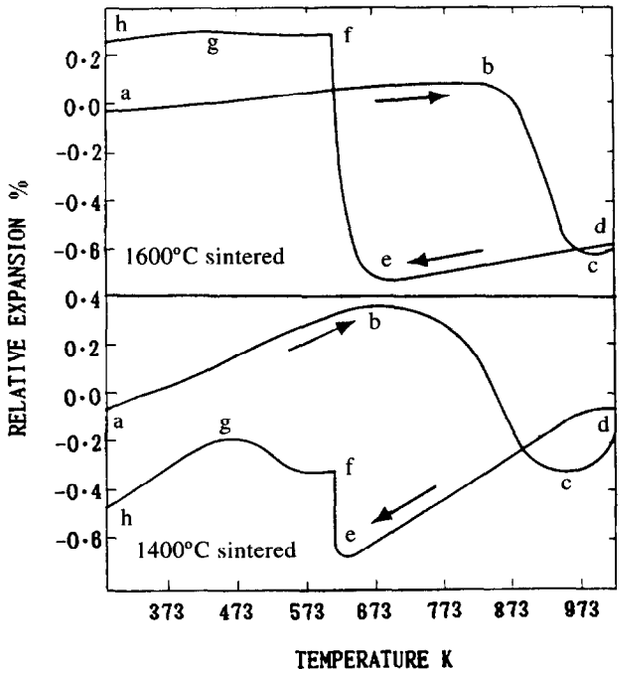

(a)

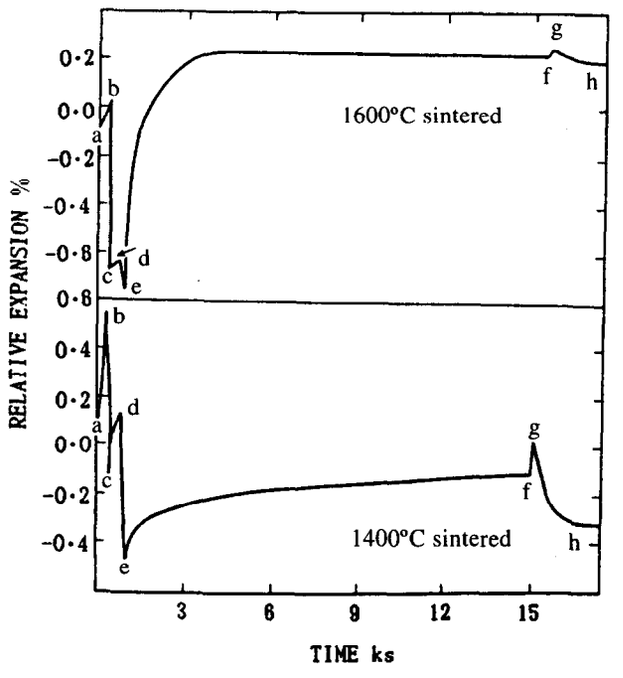

(b)

Fig. 3. Thermal expansion curves obtained at a heating and cooling rate of 100°C min^{-1} for 2Y(1600) and 2Y(1400) specimens held at 350°C for 4h : (a) expansion versus temperature ; (b) expansion versus time.

(3) Table 4 lists the value of n and transformation activation energy (Q_m) for 2Y(1600) and 2Y(1400) specimens held at different temperatures, it is clear that the value of n, the exponent in kinetics equation, is determined to be 0·88 when the holding temperature is within the range of 250–400°C and 0·81 when the holding temperature is 450°C for the 2Y(1600) specimen; For the 2Y(1400) specimen, the value of n increases with decreasing holding temperature implying that the nucleation sites might have changed with increasing holding temperature (Fig. 6).

(4) The functional relationship between ln(nk) and 1/T shown in Fig. 7 reveals the activation energy for transformation to be 18·67 KJ mol^{-1} and 41·52KJ mol^{-1} for 2Y(1600) and 2Y(1400) specimens, respectively, which indicates that the smaller the grain size,the larger the value of Q_m, and consequently the smaller the transformation rate. However,regardless of grain size, the transformation activation energy derived from kinetics data is much smaller than that necessary for lattice diffusion of oxygen ion itself, 96 KJ mol^{-1},[15] which implies that the whole process might be controlled by short-range diffusion of oxygen ions.[16] Large grain-sized material, which inevitably involves much more pre-m phase before holding, possesses smaller activation energy due to the autocatalytic effect of nucleation.[17]

3.3 Effect of grain size on incubation period

Assuming that the ideal grain boundary nucleation model fits the present case,which will be illustrated later as being at least suitable for the initial state of transformation,the isothermal transition kinetics equation can be expressed:[18]

$$f = 1 - exp\left(\frac{-A}{V} U\tau\right) \tag{2}$$

where A/V is the area of grain boundary per unit volume, U growth velocity, holding time needed for the appearance of 1% m-phase is defined as the incubation period, then:

$$\tau_{0\cdot01} = \frac{V}{AU} In \frac{1}{0\cdot99} \tag{3}$$

The grain boundary specific areas of 2Y(1600) and 2Y(1400) are presumed to be A_1/V_1 and A_2/V_2 respectively, therefore we have:

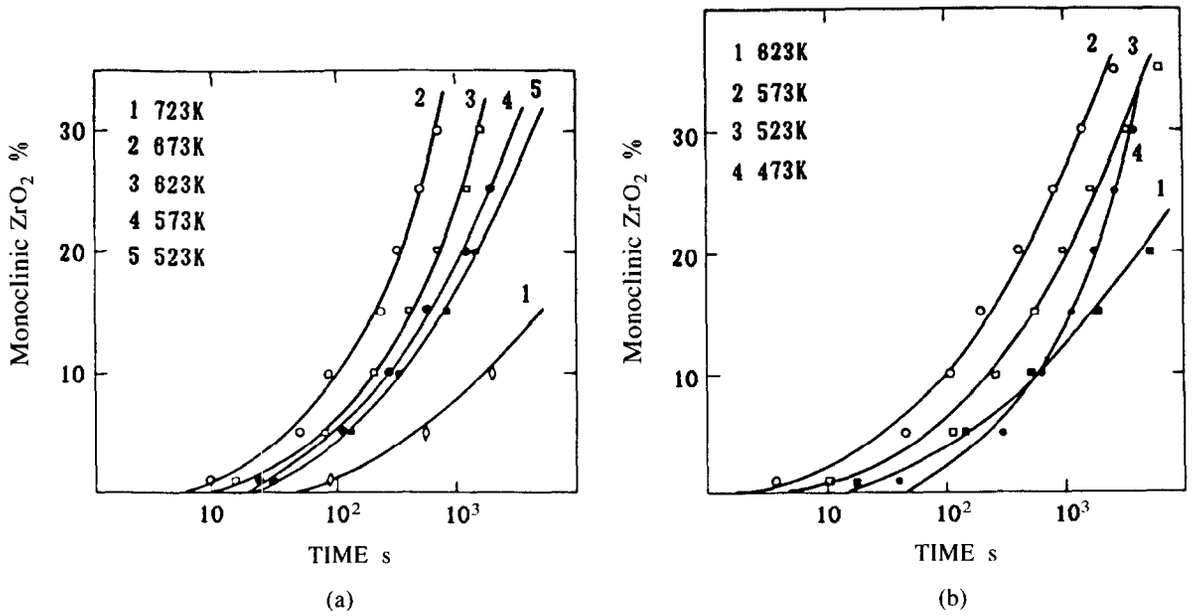

Fig. 4. Changes of the fraction of *m*-phase with holding time for 2Y(1600) and 2Y(1400) specimen held at different temperatures for 4h : (a) 2Y(1600) ; (b) 2Y(1400).

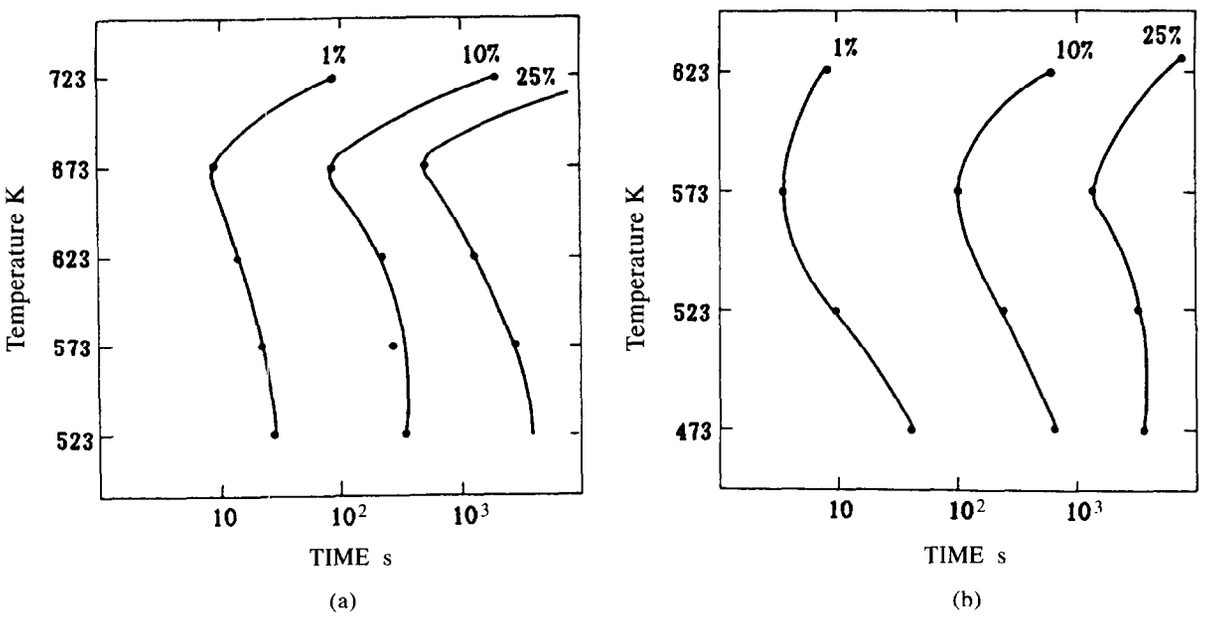

Fig. 5. Time-temperature-transformation (TTT) curves of 2Y(1600) and 2Y(1400) specimens : (a) 2Y(1600) ; (b) 2Y(1400).

Table 2. Results of thermal expansion and XRD measurements for 2Y(1600) specimens held at different temperatures for 4 h

Holding temperature (°C)	*450*	*400*	*350*	*300*	*250*
Pre-*m* phase	2·70%	18·40%	52·50%	63·46%	70·64%
Isothermal *m*-phase	12·60%	51·90%	31·70%	29·80%	24·76%
Athermal *m*-phase after holding	80·20%	26·50%	8·10%	2·88%	0
Overall *m*-phase	95·50%	96·70%	92·30%	96·20%	95·40%
Expansion prior to holding	0·0480%	0·2150%	0·6203%	0·7091%	0·8607%
Expansion during holding	0·1385%	0·6070%	0·3742%	0·3337%	0·30175
Expansion after holding	0·7622%	0·3095%	0·9580%	0·3220%	0
Overall expansion	0·9007%	1·1315%	1·0903%	1·0750%	1·1624%

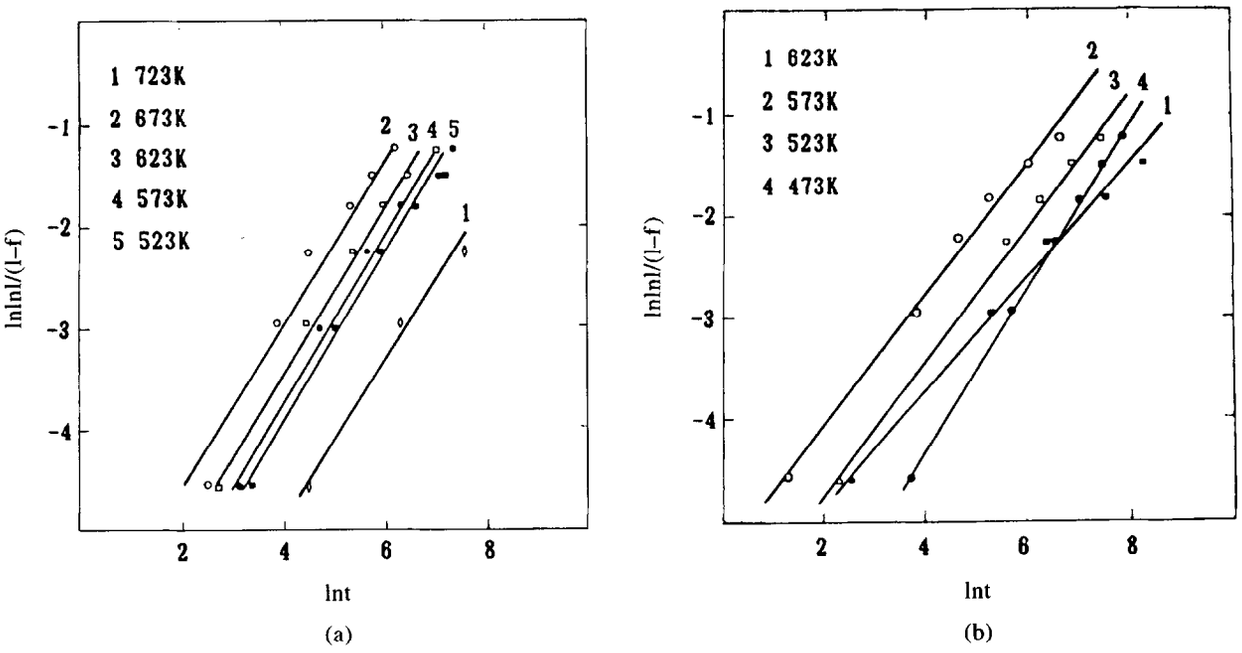

Fig. 6. Relationship between lnln1 / (1−f) and lnt for 2Y(1600) and 2Y(1400) specimens : (a) 2Y(1600) ; (b) 2Y(1400).

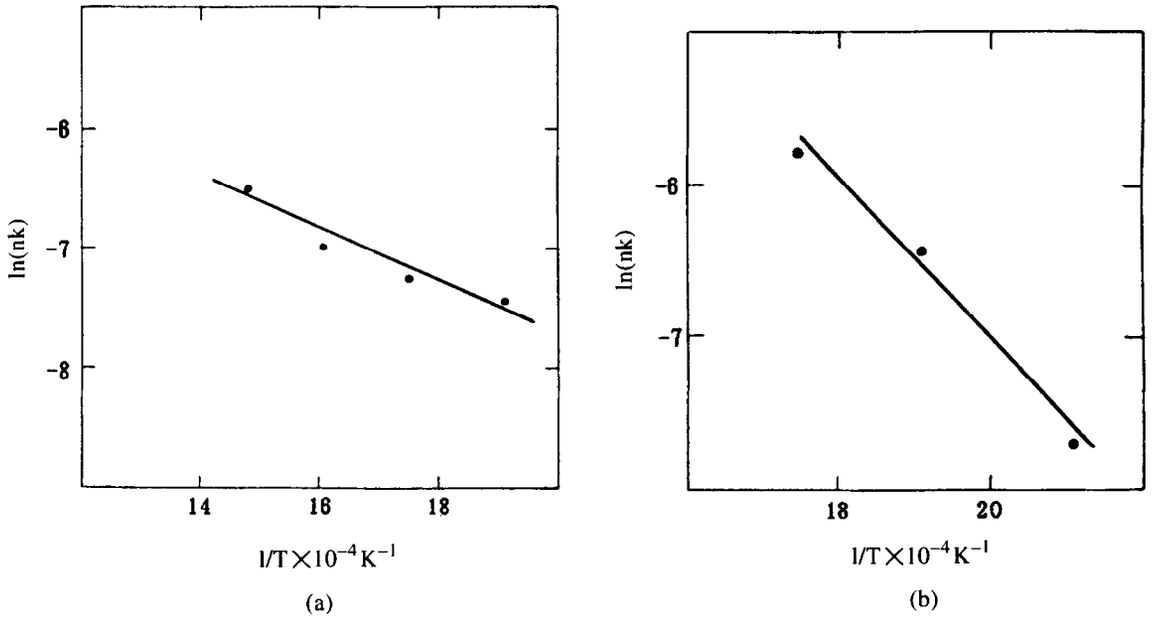

Fig. 7. Linear relationship between lnln(nk) and 1 / T for 2Y(1600) and 2Y(1400) specimens : (a) 2Y(1600) ; (b) 2Y(1400).

Table 3. Results of thermal expansion and XRD measurements for 2Y(1400) specimens held at different temperatures for 4 h

Holding temperature (°C)	*350*	*300*	*250*	*200*
Pre-*m* phase	4·30%	26·47%	41·51%	37·67%
Isothermal *m*-phase	23·20%	44·81%	39·00%	42·79%
Athermal *m*-phase after holding	30·87%	13·42%	3·19%	0·74%
Overall *m*-phase	58·40%	84·70%	89·70%	81·20%
Expansion prior to holding	0·0671%	0·4401%	0·7631%	0·66%
Expansion during holding	0·3612%	0·7453%	0·6265%	0·7497%
Expansion after holding	0·4802%	0·2232%	0·0512%	0·0129%
Overall expansion	0·9081%	1·4080%	1·4410%	1·4230%

Table 4. The value of n for 2Y(1600) and 2Y(1400) specimens held at different temperatures and transformation activation energy Q_m

Temperature (°C) / *Specimen*	*450*	*400*	*350*	*300*	*250*	*200*	$Q_m(KJmol^{-1})$
2Y(1600)	$n=0.81$	$n=0.88$	$n=0.88$	$n=0.88$	$n=0.88$		18·67
2Y(1400)			$n=0.58$	$n=0.68$	$n=0.68$	$n=0.8$	41·52

$$\frac{[\tau_{0.01}]_1}{[\tau_{0.01}]_2} = \frac{\frac{V_1}{A_1U_1}\,In\,\frac{1}{0.99}}{\frac{V_2}{A_2U_2}\,In\,\frac{1}{0.99}}. \tag{4}$$

If $U_1 = U_2$, then

$$\frac{[\tau_{0.01}]_1}{[\tau_{0.01}]_2} = \frac{V_1/A_2}{V_2/A_2}. \tag{5}$$

The shape of the grain is hypothesized to be in the form of the sphere:

$$\frac{V}{A} = \frac{\frac{4}{3}\pi r^3}{4\pi^2} = \frac{1}{3}r$$

then

$$\frac{[\tau_{0.01}]_1}{[\tau_{0.01}]_2} = \frac{r_1}{r_2} = \frac{1.47}{0.48} \approx 3.1 \geq 1$$

It is evident that if the present case conforms completely to grain boundary nucleation, the incubation period becomes shorter as the grain size is decreased, which agrees with the kinetics feature of upper-bainite in steel; the ratio of incubation periods experimentally measured at different holding temperatures as shown in Table 5 demonstrates that, though experimental values are much smaller than calculated ones, they are still higher than unity. It is noted that, in actual transformation processes, besides grain boundaries as main nucleating sites, non-Avrami phenomenon due to self-catalytic nucleation as well as nucleations at such defects as dislocations and stacking faults will lead to the occurrence of n below unity in Avrami equation, therefore, eqn (2) is only suitable for the initial state of transformation. In fact, even at the same holding temperature, growth velocity determined by both transformation activation energy (Q_m) and driving force (ΔG_V) is different for samples with different grain size. Transformation rate dependent on activation energy (Q_m) is large and starting temperature for t→m transformation (M_s) is high when grain size is large, which leads to a larger growth velocity. Specifically speaking, when grain size is small, although incubation period is short, the transformation rate thereafter is small; When grain size is large, although incubation period is long, the transformation rate thereafter is large, which results in large volume fraction of isothermal m-phase produced. Therefore, the incubation period is determined by critical nucleation energy barrier and density of nucleation sites; transformation rate depends on activation energy for transformation (Q_m) and 'nose' temperature of the TTT curve is determined by M_s point.

3.4 Interpretation of TTT curve

The generation of the TTT curve with a C-shape is undoubtedly attributable to at least two contradicting factors responsible for the nucleation and growth of m-phase. Grain boundaries are the most favourable nucleation sites compared with other defects. For simplicity, we analyse the thermodynamics of nucleation at grain boundaries for the t→m transformation.

Assume λ_1,λ_2 to be the interface energy of t/m and grain boundary energy of t/t, respectively; A_1 and A_2 represent the area of the t/m interface and t/t grain boundary, respectively; ΔE is the change in strain energy associated with transformed m-phase and surrounding t-phase; ΔG_v, is the change of chemical free energy between t and m phases, r and V are the radius and volume of the nucleus, respectively. When the transformation occurs, the variation of free energy can be expressed as:[18]

$$\Delta G = \gamma_1 A_1 - \gamma_2 A_2 - \Delta G_v V + \Delta E V \tag{6}$$

where

$$A_1 = \pi\left[1 - \left(\frac{\gamma_2}{\gamma_1}\right)^2\right]r^2$$

$$A_2 = 4\pi\left[1 - \left(\frac{\gamma_2}{\gamma_1}\right)^2\right]r^2$$

$$V = \frac{2}{3}\pi\left[2 - 3\left(\frac{\gamma_2}{\gamma_1}\right) + \left(\frac{\gamma_2}{\gamma_1}\right)^3\right]r^3.$$

Because γ_1, γ_2 are constants, a, b, c represent coefficients in front of r^2 and r^3, that is:

Table 5. Incubation period for 2Y(1600) and 2Y(1400) specimens held at different temperatures

I_pT Specimen	350°C	300°C	250°C
2Y(1600)	18·4 s	20·2 s	28·2 s
2Y(1400)	9·8 s	7·8 s	11·2 s
Ratio of I_p	1·8	2·6	2·5

$$\pi\left[1-\left(\frac{\gamma_2}{\gamma_1}\right)^2\right]=\mathrm{a},\ 4\pi\left[1-\left(\frac{\gamma_2}{\gamma_1}\right)^2\right]=\mathrm{b}$$

$$\frac{2}{3}\pi\left[2-3\left(\frac{\gamma_2}{\gamma_1}\right)+\left(\frac{\gamma_2}{\gamma_1}\right)^3\right]=\mathrm{c}$$

then eqn (6) is changed to

$$\Delta G=\gamma_1 ar^2-\gamma_2 br^2-\Delta G_v cr^3+\Delta Ecr^3 \quad (7)$$

take

$$\frac{\partial\Delta G}{\partial r}=0$$

the critical radius of nucleus can be expressed as:

$$r*=\frac{2(\gamma_1 a-\gamma_2 b)}{3c(\Delta G_v-\Delta E)} \quad (8)$$

the critical nucleation barrier is written as:

$$\Delta G^*=r^{*2}2(\gamma_1 a-\gamma_2 b)/3=M/(\Delta G_v-\Delta E)^2 \quad (9)$$

where M is a proportional constant.

Because

$$\Delta G_v=\Delta T\times\frac{\Delta H}{T_0},\ \Delta H=T_0-T$$

where ΔH is enthalpy of t→m transformation, T_0 the equilibrium temperature between t and m phases, per unit time, per unit volume, the number of stable nuclei can be written as:[18]

$$I=\omega A\exp(-\Delta G^*/kT)\exp(-Q_m/kT) \quad (10)$$

where ω is the frequency of ion vibration, A is the area of grain boundaries per unit volume, and Q_m the activation energy for the diffusion of oxygen ion. In eqn (10), the term $\exp(-Q_m/kT)$ represents the mobility of atoms and decreases with decreasing temperature, while ΔG^* in $\exp(-\Delta G^*/kT)$ is a relatively complicated function of temperature:

$$\exp(-\Delta G^*/kT)=\exp[-M'/(\Delta G_v-\Delta E)] \quad (11)$$

where M' is a proportional constant

$$(\Delta G_v-\Delta E)^2T=$$
$$[(\Delta T\times\Delta H-\Delta E\times T_0)/T_0]^2(T_0-\Delta T)=B \quad (12)$$

then

$$\frac{\partial(1/B)}{\partial(\Delta T)}=-2\left(\frac{\Delta T\times\Delta H-\Delta E\times T_0}{T_0}\right)^{-3}\times\frac{\Delta H}{T_0}(T_0-\Delta T)^{-1}$$
$$+\left(\frac{\Delta T\times\Delta H-\Delta E\times T_0}{T_0}\right)^{-2}\times(T_0-\Delta T)^{-2} \quad (13)$$

equalize eqn (13) to zero, then we obtain

$$\Delta T=\frac{T_0(2\Delta H+\Delta E)}{3\Delta H} \quad (14)$$

Substitute
$\Delta H=282{\cdot}61\ \mathrm{J\,cm^{-3}}$ [19] and $\Delta E=17{\cdot}98\ \mathrm{J\,cm^{-3}}$ [19] into eqn (14) and we get

$$\Delta T\approx\frac{2}{3}T_0.$$

According to dilation result, T_0 is taken as 773 K and remains unchanged with sintering temperature.

Then $\Delta T=515$ K, when $\Delta T<515$ K, i.e. $(2/3)T_0$, the following expression exists

$$\partial[\exp(-\Delta G^*/kT)]/\partial(\Delta T)>0. \quad (15)$$

It is observed that the holding temperatures are in range of $\Delta T<515$ K, therefore, the term $\exp(-\Delta G^*/kT)$ increases with decreasing temperature. In addition, besides grain boundaries, nuclei can also form at such defects as dislocations and stacking faults with an increasing degree of supercooling. In view of this, A in eqn (10) is regarded as an effective density of heterogeneous nucleating sites and increases with decreasing temperature. As reflected in the Avrami eqn, the value of n increases initially with decreasing temperature and becomes almost constant when temperature is further decreased due to the saturation of nucleating sites. The nucleation rate firstly increases then decreases with decreasing temperature as schematically shown in Fig. 8(a). If the growth of m-phase is considered to be controlled by movement of interface, when the

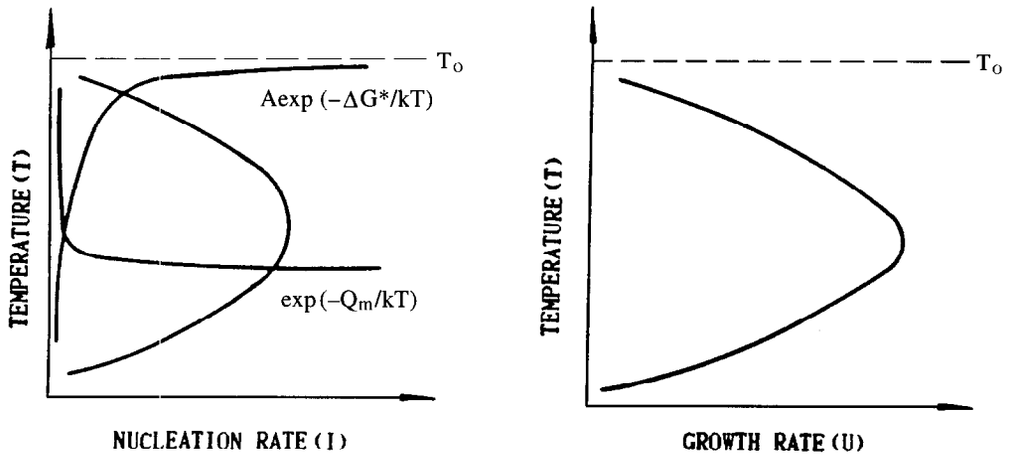

Fig. 8. Schematic presentations indicating : (a) changes of nucleation rate with temperature and (b) changes of growth rate with temperature for *m*-phase during t→m transition.

driving force is relatively small, the rate of *t*/*m* interface movement can be written as:[20]

$$U = (\omega\delta/k)(\Delta G_v/T)\exp(-Q_m/kT) \qquad (16)$$

when the driving force is relatively large, U can be expressed as[20]

$$U = \omega\delta\exp(-Q_m/kT) \qquad (17)$$

where δ is the thickness of the *t*/*m* interface. The rate of interface propagation is controlled by both ΔG_v and $\exp(-Q_m/kT)$, when the holding temperature is high ΔG_v becomes a controlling factor; when the holding temperature is low, $\exp(-Q_m/kT)$ becomes a controlling factor. Therefore, U initially increases then decreases with decreasing temperature as shown in Fig. 8(b). In conclusion, both nucleation and growth are responsible for the presence of the TTT curve with C-shape. The increase in the fraction of m-phase can be attributed to both the propagation of original plates and the formation of new plates, and nucleation and growth are kinetically controlled by the diffusion. The effect of self-catalytic nucleation is obvious in that the transformation cannot proceed to completion with *t* + *m* dual phase as the final microstructure because of large constraints imposed on the parent phase.

3.5 TEM observation of microstructure

TEM photographs of the coarse-grained specimen shown in Fig. 9 reveal that most of the grains possess the microstructure of either *m*-phase or *t* plus *m* dual phase. Microcracks accompanying t→m transformation distribute not only at the grain boundaries of original *t*-phase, but also at the intersection of twinned *m*-phase variants [Fig. 9(a)]. Coexistence of *t* plus *m* dual phase in the same grain as shown in Fig. 9(b) indicates that *m*-phase plates nucleate preferentially at the grain boundary and grow inward across the grain during which they are impeded by growing m phase plates from

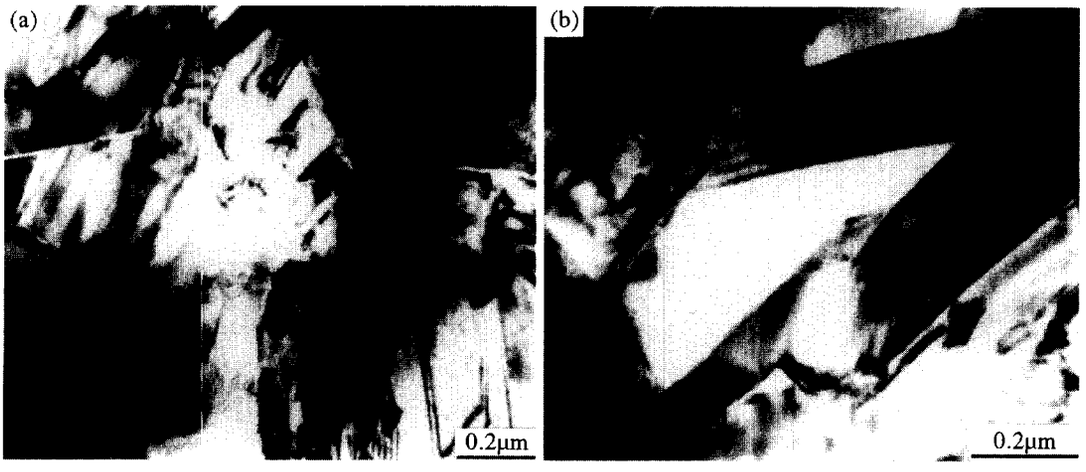

Fig. 9. TEM photographs of 2Y(1600) specimen : (a) microcracks at grain and twinned interfaces (indicated by arrows); (b) *t* and *m* phases coexist within one grain.

the opposite direction and thus terminate inside the original t-phase grain. In contrast, most of the grains exist in the form of either t-phase or t plus m dual phase rather than solely m-phase for the fine-grained specimen as shown in Fig. 10, which agrees with kinetics results in that stability of t-phase can be improved by refining the grains. Previous studies[21] show that there exists a critical diameter (D_c) for a certain type of $ZrO_2(Y_2O_3)$ ceramic and when the grain size of t-phase is larger than D_c, $t \rightarrow m$ transformation will occur and microstructure of the grain will consist of m-phase, otherwise, the grain will be in the form of t-phase. In addition, residual stresses arising from anisotropy of the thermal expansion coefficient of t-phase scale with grain size and residual stresses are always thought to facilitate t→m transformation. Finally, the strength of material increases with decreasing grain size, which results in the fact that mechanisms of twinning and microcracking to relax strain energy concurrent with transformation are difficult to operate. Figures 10(a) and (b) show the bright field image of t-phase grains of the 2Y(1400) specimen and diffraction pattern of [111] direction, respectively. All the grains are in the form of t-phase and sizes of grains vary greatly. Figure 10(c) shows the case in which two plates of m-phase nucleate simultaneously at the grain boundaries and propagate across the grain to the opposite side and the growing process is thus inhibited, indicating that grain boundaries are both preferential sites for m-phase nucleation and final places for m-phase growth. It is understood that grain boundaries are radiating sources of dislocations, and at the same time, they can absorb dislocations within the grain. When misfit dislocations at t/m interface are absorbed, growth of m-phase in the longitudinal direction thus stops. It is observed that growing velocity in the longitudinal direction is much faster than that in the transverse direction. Orientational relationship between t and m phases shown in Fig. 10(d) is indexed as follows: $(100)t//(100)m$ $[013]t//[013]m$.

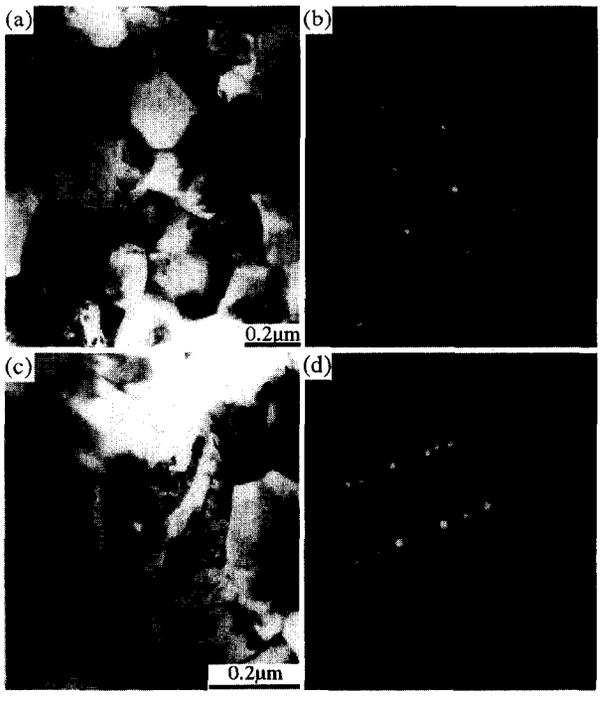

Fig. 10. TEM photographs of 2Y(1400) specimen : (a) bright field image showing only t phase grains; (b) diffraction pattern from [111] direction; (c) bright field image showing coexistence of t plus m phases; (d) diffraction pattern with orientation relationship between t and m phases indexed as $[013]_t$ // $[013]_m$ $(100)_t$ // $(100)_m$.

4 Conclusions

(1) Grain size has an obvious effect on kinetics of isothermal t→m transformation in ZrO_2 (Y_2O_3) ceramics. With decreasing grain size of t-phase, the 'nose' temperature of the time-temperature-transformation (TTT) curve is decreased, incubation period is shortened and the transformation rate afterwards is decreased as well as incompleteness of transformation being enhanced.

(2) The occurrence of TTT curve with a C-shape has been rationalized in terms of thermodynamic analysis with the hypothesis that grain boundaries are the most favourable sites for m-phase nucleation.

(3) Phase constituents vary with grain size. For coarse-grained specimens, single m-phase or t plus m dual phase occupies the original t-phase grain; For fine-grained specimens, single t-phase or t plus m dual phase occupies the original t-phase grain. Stability of t-phase increases with decreasing grain size.

References

1. Garvie, R. C., Hughan, R. R. and Pascoe, R. T., *Nature*, 1975, **258**, 703.
2. Evans, A. G. and Heuer, A. H., *Journal of Am. Ceram. Soc.*, 1980, **63**, 241.
3. Memeeking, R. M. and Evans, A. G., *Journal of Am. Ceram. Soc.*, 1982, **65**, 242.
4. Zhu, W. Z., Lei, T. C. and Zhou, Y., *Journal of Mat. Sci.*, 1993, **28**, 6479.
5. Farmer, S. C., Heuer, A. H., Hannink, R. H. J., *Journal of Am. Ceram. Soc.*, 1987, **70**, 431.
6. Nakanishi, N. and Shigematsu, T., *Zirconia Ceram.*, 1986, **8**, 71.
7. Nakanishi, N. and Shigematsu, T., *Mater. Trans. Jpn. Inst. Met.*, 1991, **32**, 778.
8. Nakanishi, N. and Shigematsu, T., *Mater. Trans. Jpn. Inst. Met.*, 1992, **33**, 318.
9. Behrens, G., Dransmann, G. W. and Heuer, A. H., *Journal of Am. Ceram. Soc.*, 1993, **76**, 1025.

10. Tsubakino, T., Hamamoto, M. and Nozato, R., *Journal of Mater. Sci.*, 1991, **26**, 5521.
11. Subbara, E. C., Science and Technology of Zirconia. In *Advances in Ceramics*, Vol. 3, ed. A. G. Evans, American Ceramics Society, Columbus, Ohio, 1981, p 1.
12. Bansal, G. K. and Heuer, A. H., *Acta. Metall.*, 1972, **20**, 1281.
13. Bansal, G. K. and Heuer, A. H., *Acta. Metall.*, 1974, **22**, 409.
14. Garvie, R. C. and Nicholson, P. S., *Journal of Am. Ceram. Soc.*, 1972, **55**, 303.
15. Tsubakino, T., Sodona, K. and Nozato, R., *Journal of Mater. Sci. Lett.*, 1993, **12**, 196.
16. Zhu, W. Z., Lei, T. C., Zhou, Y. and Ding, Z. S., *Mater. Chem. Phys.*, 1996, **44**, 67.
17. Zhu, W. Z. and Yan, M., *Journal of Mater. Sci. Lett.*, 1996, **15**, 846.
18. Xu, Z. Y., Principles of Transformation, *Science Publisher*, 1981 (in Chinese).
19. Chen, I. W. and Chiao, Y. H., Acta. Metall., 1983, **31**, 1627.
20. He, Z. S., Introduction to Physical Metallurgy, *Shanghai Science and Technology Publisher*, 1982, p. 69 (in Chinese).
21. Hanlyn-Harris, J. H. and St. John, D. H., *Mat. Sci. For.*, 1988, **34-36**, 141.